

## Nonlinearity in the high-electric-field piezoelectricity of epitaxial BiFeO<sub>3</sub> on SrTiO<sub>3</sub>

Pice Chen, Rebecca J. Sichel-Tissot, Ji Young Jo, Ryan T. Smith, Seung-Hyub Baek et al.

Citation: *Appl. Phys. Lett.* **100**, 062906 (2012); doi: 10.1063/1.3683533

View online: <http://dx.doi.org/10.1063/1.3683533>

View Table of Contents: <http://apl.aip.org/resource/1/APPLAB/v100/i6>

Published by the [American Institute of Physics](#).

---

### Related Articles

Characteristics of thickness-shear modes excited by two-layer piezoelectric film in acoustic sensors

*J. Appl. Phys.* **111**, 033504 (2012)

Surface effects on the wrinkling of piezoelectric films on compliant substrates

*J. Appl. Phys.* **110**, 114303 (2011)

Thickness effect on nanoscale electromechanical activity in Pb(Mg<sub>1/3</sub>Nb<sub>2/3</sub>)O<sub>3</sub>-PbTiO<sub>3</sub> thin films studied by piezoresponse force microscopy

*J. Appl. Phys.* **110**, 104101 (2011)

Harmonic modulation behavior in lead lanthanum zirconate titanate ceramics

*J. Appl. Phys.* **110**, 074108 (2011)

Nitrogen [N]-incorporated ZnO piezoelectric thin films and their application for ultra-small film bulk acoustic wave resonator device fabrication

*J. Appl. Phys.* **110**, 074101 (2011)

---

### Additional information on *Appl. Phys. Lett.*

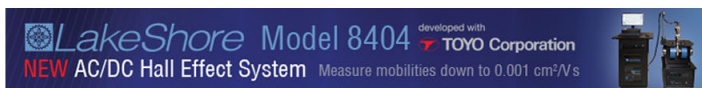
Journal Homepage: <http://apl.aip.org/>

Journal Information: [http://apl.aip.org/about/about\\_the\\_journal](http://apl.aip.org/about/about_the_journal)

Top downloads: [http://apl.aip.org/features/most\\_downloaded](http://apl.aip.org/features/most_downloaded)

Information for Authors: <http://apl.aip.org/authors>

## ADVERTISEMENT



## Nonlinearity in the high-electric-field piezoelectricity of epitaxial BiFeO<sub>3</sub> on SrTiO<sub>3</sub>

Pice Chen,<sup>1</sup> Rebecca J. Sichel-Tissot,<sup>1,a)</sup> Ji Young Jo,<sup>1,b)</sup> Ryan T. Smith,<sup>1</sup> Seung-Hyub Baek,<sup>1</sup> Wittawat Saenrang,<sup>1</sup> Chang-Beom Eom,<sup>1</sup> Osami Sakata,<sup>2,c)</sup> Eric M. Dufresne,<sup>3</sup> and Paul G. Evans<sup>1,d)</sup>

<sup>1</sup>Department of Materials Science and Engineering and Materials Science Program, University of Wisconsin, Madison, Wisconsin 53706, USA

<sup>2</sup>Japan Synchrotron Radiation Research Institute/SPring-8, Kouto, Sayo 679-5198, Japan

<sup>3</sup>Advanced Photon Source, Argonne National Laboratory, Argonne, Illinois 60439, USA

(Received 3 January 2012; accepted 21 January 2012; published online 10 February 2012)

The piezoelectricity of a multiferroic BiFeO<sub>3</sub> thin film deviates from its low-field linear response in electric fields higher than 150 MV/m. Time-resolved synchrotron x-ray microdiffraction reveals a low-field piezoelectric coefficient of 55 pm/V and a steeper increase in strain at higher fields, with an effective piezoelectric coefficient of 86 pm/V. The strain reaches 2% at 281 MV/m, a factor of 1.3 higher than expected based on an extrapolation from low fields. The peak intensity of the BiFeO<sub>3</sub> (002) Bragg reflection decreases throughout the high-electric-field regime, accompanied by increased diffuse scattering, consistent with lattice softening near a field-induced phase transition. © 2012 American Institute of Physics. [doi:10.1063/1.3683533]

High electric field phenomena are crucially important to the fundamental properties and applications of electronic materials based on thin films and nanostructures, where external voltages can easily lead to fields higher than 100 MV/m. In complex oxides, such as the multiferroic BiFeO<sub>3</sub>, high electric fields have the potential to modify electronic and electromechanical properties via the nonlinear field-dependence of dielectric susceptibility and through field-induced structural phase transitions.<sup>1,2</sup> Calculations show that a tetragonal phase of BiFeO<sub>3</sub> can be energetically favorable in comparison with the bulk rhombohedral phase when an electric field is applied along a pseudocubic ⟨001⟩ crystallographic direction.<sup>2</sup> Distinct piezoelectric, dielectric, and mechanical properties are a universal consequence of the softening of the lattice near such phase transitions.<sup>3,4</sup> Enhanced piezoelectricity has been reported in BiFeO<sub>3</sub> thin films in which large compressive biaxial strain or doping with rare earths places the system near the structural phase transition.<sup>5,6</sup> Jang *et al.*<sup>7</sup> report that a strain-induced polarization rotation mechanism is responsible for a large change in the out-of-plane polarization of (001) BiFeO<sub>3</sub> with biaxial strain, while the spontaneous polarization itself remains almost constant. The field-driven rhombohedral-to-tetragonal phase transition in BiFeO<sub>3</sub> can be produced by a moderate electric field of 176 MV/m in layers grown under epitaxial constraints where rhombohedral and tetragonal phases coexist at zero field.<sup>8</sup> When epitaxial conditions yield purely rhombohedral BiFeO<sub>3</sub>, however, the rhombohedral structure

is more stable and the production of the field-induced tetragonal phase has not been experimentally demonstrated.

In this letter, we show that a rhombohedral BiFeO<sub>3</sub> layer exhibits electromechanical phenomena in high electric fields that are consistent with the proximity of the rhombohedral-to-tetragonal phase transition. The piezoelectric strain measured using time-resolved x-ray diffraction is proportional to the applied electric field up to 150 MV/m, and increases more rapidly at higher fields. The diffuse component of the scattered x-rays increases at high electric fields, and the peak intensity of Bragg reflections simultaneously decreases. The increase of piezoelectricity and diffuse scattering are consistent with the softening of phonon modes in BiFeO<sub>3</sub> at high electric fields near the phase transition. The fields reached in these experiments, however, are not sufficient to yield a transition to the tetragonal phase.

A 54 nm-thick BiFeO<sub>3</sub> layer with (001)-pseudocubic orientation was prepared on a 50 nm-thick single crystal SrRuO<sub>3</sub> bottom electrode on a (001)-oriented SrTiO<sub>3</sub> substrate by off-axis magnetron sputtering.<sup>9,10</sup> Thin-film capacitors were formed by depositing Pt top electrodes with diameters of 25 and 50 μm onto the BiFeO<sub>3</sub> layer. Applying short-duration voltage pulses produces electric fields that can briefly exceed the low-frequency breakdown field without damaging the sample.<sup>11</sup> Time-resolved x-ray microdiffraction experiments were conducted at station 7IDB of the Advanced Photon Source (APS, Argonne, IL) and at beamline BL13XU at SPring-8 (Harima, Japan).<sup>12</sup> At the APS, 10 keV photons were focused to a spot size of 100-200 nm with a Fresnel zone plate and diffracted x-rays were detected by either an avalanche photodiode (APD) or a pixel array detector. At Spring-8, 12.3 keV photons were focused to 2.5 μm with a refractive lens and diffracted x-rays were detected using an APD.

Fig. 1(a) shows the evolution of the BiFeO<sub>3</sub> (002) Bragg reflection during a 12 ns-duration electric field pulse with a

<sup>a)</sup>Present address: Materials Science and Engineering, Drexel University, Philadelphia, Pennsylvania 19104, USA.

<sup>b)</sup>Present address: School of Materials Science and Engineering, Gwangju Institute of Science and Technology, Gwangju 500-712, Korea.

<sup>c)</sup>Present address: Synchrotron X-ray Station at SPring-8, National Institute for Materials Science, Kouto, Sayo, Hyogo 679-5148, Japan.

<sup>d)</sup>Electronic mail: evans@engr.wisc.edu.

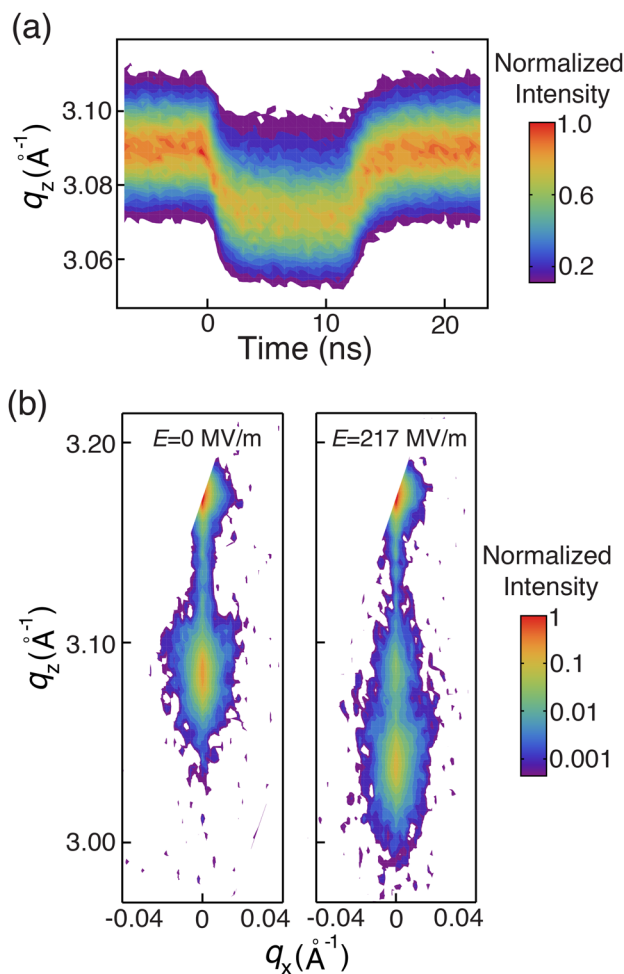


FIG. 1. (Color online) (a) Intensity near the BiFeO<sub>3</sub> (002) Bragg reflection as a function of time and wavevector  $q_z$  during an electric field pulse with magnitude 102 MV/m and duration 12 ns. (b) Maps of diffracted intensity as a function of  $q_z$  and in-plane wavevector  $q_x$  near the BiFeO<sub>3</sub> (002) Bragg reflection at zero field (left) and 217 MV/m (right). The SrRuO<sub>3</sub> (002) reflection at  $q_z = 3.173 \text{ \AA}^{-1}$  is cut off at high  $q_z$  and low  $q_x$  as a result of the angular range of the measurement.

magnitude of 102 MV/m. The diffracted intensity shifts to lower wavevector  $q_z$  during the electric field pulse due to the expansion of the lattice along the surface-normal  $z$  direction, and returns to its initial value when the field is turned off. The initial piezoelectric expansion has an exponential time dependence with a time constant of 1.4 ns arising from the charging of the BiFeO<sub>3</sub> capacitor. The resistive factor in the charging time constant is dominated by the sheet resistance of the SrRuO<sub>3</sub> bottom electrode. Based on the time response observed in Fig. 1(a), a fixed delay long after the initial expansion was chosen to perform a structural study of BiFeO<sub>3</sub> under a range of applied electric fields.

Two-dimensional slices of reciprocal space acquired before the application of the electric field and at 17 ns after the onset of a 20-ns pulse with magnitude  $E = 217 \text{ MV/m}$  are shown in Fig. 1(b). The center of the BiFeO<sub>3</sub> (002) reflection shifts from  $q_z = 3.084 \text{ \AA}^{-1}$  at  $E = 0$  to  $q_z = 3.039 \text{ \AA}^{-1}$  at  $E = 217 \text{ MV/m}$ , a tensile strain of 1.46%. There is no change of the apparent in-plane wavevector  $q_x$  of the BiFeO<sub>3</sub> reflection between  $E = 0$  and  $E = 217 \text{ MV/m}$ , Fig. 1(b), indicating that the BiFeO<sub>3</sub> layer is not tilted during the applied electric fields. A secondary peak at the zero-field

wavevector of the (002) reflection, as at  $E = 178 \text{ MV/m}$  in Fig. 2(a) and  $E = 217 \text{ MV/m}$  in Fig. 1(b), arises from the illumination of an area of the sample outside the top electrode by an unfocused portion of the incident x-ray intensity.

The electric field dependence of the piezoelectric strain was measured using a series of intensity vs.  $q_z$  scans similar to Fig. 2(a). The piezoelectric strain is plotted in Fig. 2(b) as a function of the magnitude of the electric field pulses. In the low-field regime, below 150 MV/m, the strain is proportional to  $E$ , with a piezoelectric coefficient of 55 pm/V. The linearity of this response and the value of the piezoelectric coefficient are consistent with previous observations of coefficients of 50-60 pm/V in both bulk BiFeO<sub>3</sub> ceramics and in rhombohedral thin films.<sup>13-15</sup> The strain deviates from the linear piezoelectricity in electric fields higher than 150 MV/m. At the highest field we have probed,  $E = 281 \text{ MV/m}$ , the piezoelectric strain in the BiFeO<sub>3</sub> thin film is 2.04%, a factor of 1.3 larger than the value predicted by extrapolating the low- $E$  piezoelectric coefficient.

The peak intensity of the BiFeO<sub>3</sub> (002) Bragg reflection is reduced at high  $E$ , and the diffuse intensity near the Bragg peak increases. Fig. 3(a) shows a scan through the BiFeO<sub>3</sub> (002) reflection along the [110] direction of reciprocal space, illustrating the relative increase in diffuse scattering between  $E = 0$  and  $E = 230 \text{ MV/m}$ . Note that the peak intensity of the Bragg reflection in Fig. 3(a) is normalized to 1 for each electric field to facilitate the comparison of the diffuse components. The variation of the peak intensity of the (002) reflection is shown as a function of  $E$  in Fig. 3(b). At higher

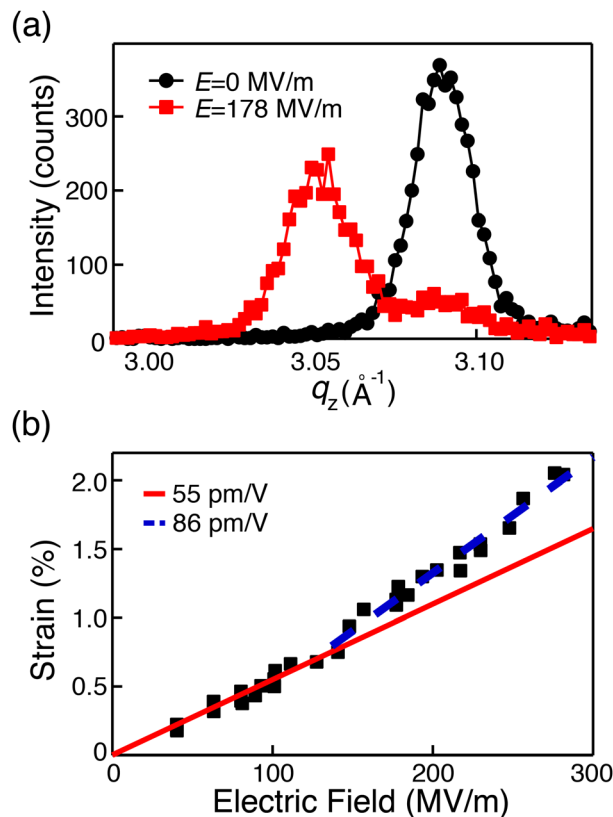


FIG. 2. (Color online) (a) Intensity vs. wavevector  $q_z$  for the (002) BiFeO<sub>3</sub> Bragg reflection at zero field (circles) and 178 MV/m (squares). (b) Piezoelectric strain as a function of electric field. The solid and dashed lines are linear fits for electric fields less than 150 MV/m and greater than 150 MV/m, respectively.

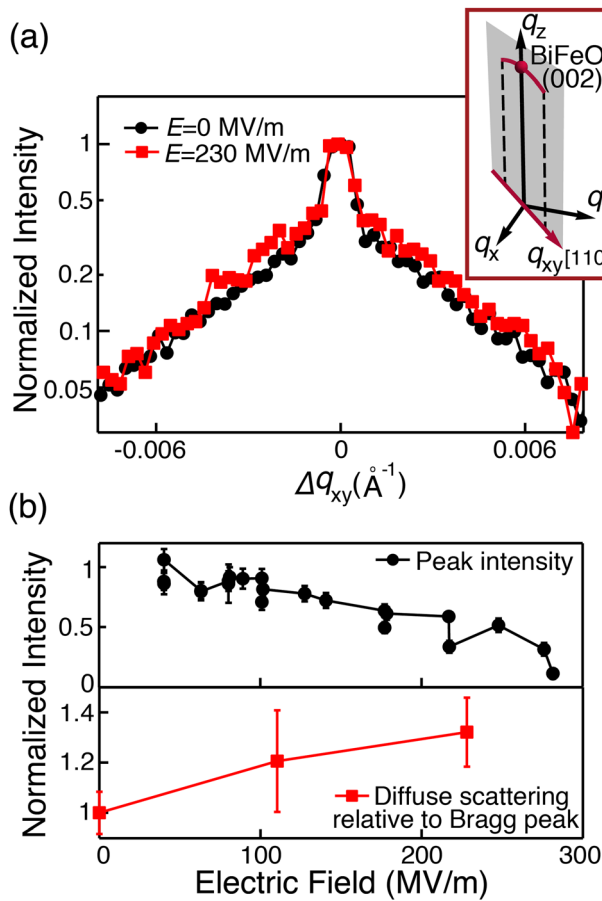


FIG. 3. (Color online) (a) Intensity as a function of the in-plane wavevector  $\Delta q_{xy}$  for the  $\text{BiFeO}_3$  (002) Bragg reflection at zero field (circles) and 230 MV/m (squares). Here,  $\Delta q_{xy}$  is the projection of the scattering wavevector onto the pseudocubic [110] direction (inset). (b) The peak intensity of  $\text{BiFeO}_3$  (002) Bragg reflection normalized to its zero-field value (upper panel), and the ratio of the diffuse and Bragg components of the scattering integrated over the ranges specified in the text (lower panel). The error bars are derived from counting statistics in the intensity integration.

$E$ , the peak intensity of the Bragg reflection falls to 30% of its zero-field value at an electric field of 281 MV/m. The angular width of the Bragg reflection is unchanged in the high fields.

The relative intensities of the diffuse scattering and Bragg reflection can be quantified by partitioning the line of reciprocal space shown in Fig. 3(b) into two regions: a Bragg region in which the projection of the wavevector onto [110],  $\Delta q_{xy}$ , is less than  $2.5 \times 10^{-4} \text{\AA}^{-1}$ , and a diffuse region with  $\Delta q_{xy}$  between 0.002 and  $0.008 \text{\AA}^{-1}$ . The ratio of the integrated intensities in these two regions as a function of  $E$  is shown in Fig. 3(b). At  $E=230$  MV/m, the intensity of the diffuse scattering in this narrow one-dimensional section of reciprocal space has increased by 30% relative to the Bragg peak. Integration over the full three-dimensional volume of reciprocal space near the  $\text{BiFeO}_3$  (002) reflection shows that the total scattered intensities at  $E=0$  and  $E=217$  MV/m are equal within 6%. The variation in total intensity is smaller than the systematic uncertainty associated with the experimental integration over reciprocal space and we thus conclude that the intensity is conserved within the limits of the precision of our experiment. The conservation of the total intensity is consistent with a redistribution of scattered intensity from the Bragg peak into the diffuse component.

The enhanced piezoelectricity, reduced Bragg-peak intensity, and increased diffuse scattering at high fields in  $\text{BiFeO}_3$  are consistent with the softening of phonon modes in the proximity of the rhombohedral-to-tetragonal phase transition. Increased piezoelectricity is caused by the divergence of both the dielectric and electromechanical properties, as in low-field measurements of systems with compositions near phase boundaries.<sup>3</sup> The piezoelectric coefficient of  $\text{BiFeO}_3$  is as large as 115 pm/V in thin films with a mixture of rhombohedral and tetragonal phases.<sup>5</sup> In the present case, the effective piezoelectric coefficient for differential increases in electric fields above 150 MV/m is 86 pm/V, as shown in Fig. 2(b). A similar experiment has probed the piezoelectricity of tetragonal  $\text{Pb}(\text{Zr}_{0.2}\text{Ti}_{0.8})\text{O}_3$ , a composition firmly on the tetragonal side of the morphotropic phase boundary in that system.<sup>11</sup> Because the rhombohedral-to-tetragonal transition was not available via a tensile expansion of  $\text{Pb}(\text{Zr}_{0.2}\text{Ti}_{0.8})\text{O}_3$ , neither the decrease in the peak intensity of the Bragg reflection nor the large increase in piezoelectricity was observed for fields up to 500 MV/m.<sup>11</sup>

The increase in the diffuse component of the scattered x-ray intensity is consistent with increased thermal diffuse scattering from a larger thermally excited population of phonons in modes softened by the proximity of the phase transition. The x-ray diffuse scattering intensity increases near structural phase transitions, as previously observed in  $\text{SrTiO}_3$  and  $\text{TiSe}_2$ .<sup>16,17</sup> Unstable soft modes in phase transitions between the  $\text{BiFeO}_3$  rhombohedral and tetragonal phases are near-zone-center phonon modes that can be expected to contribute to diffuse scattering in the range shown in Fig. 3(a).<sup>18</sup>

The increased high-field piezoelectricity of  $\text{BiFeO}_3$  occurs at lower electric fields than that which would be required to drive the  $\text{BiFeO}_3$  layer through the field-induced phase transition. The results here are similar to the different low- and moderate-field regimes of the piezoelectricity of the relaxor ferroelectric  $\text{Pb}(\text{Zn,Nb})\text{O}_3$ - $\text{PbTiO}_3$  system, these termed the A and B stages, and thought to correspond to the proximity of the tetragonal phase.<sup>19</sup> In the event of a field-induced phase transition between rhombohedral and tetragonal phases, one would also expect to observe the appearance of diffracted intensity from the tetragonal phase. We have searched for additional reflections at  $E=230$  MV/m in the reciprocal space region where diffraction from the tetragonal phase has been reported, and found no sign of the tetragonal structure. We conclude that the field-induced phase transition requires an electric field higher than the maximum field we have probed. An alternative explanation based on populations of polarization domains switching at high fields, as reported for  $\text{Pb}(\text{Zr,Ti})\text{O}_3$ ,<sup>20</sup> would require a large population of small polarization domains, but cannot be completely ruled out.

Previous studies of  $\text{BiFeO}_3$  layers grown on substrates inducing large compressive strains can be used to estimate the field required for a rhombohedral-to-tetragonal transition in  $\text{BiFeO}_3$  on  $\text{SrTiO}_3$ . A mixture of tetragonal and rhombohedral structures has been observed at a tetragonality of 1.07.<sup>8</sup> Expanding a  $\text{BiFeO}_3$  thin film on  $\text{SrTiO}_3$  to this point requires an out-of-plane strain of 2.5%. By slightly extrapolating our measurements, we predict that this 2.5% strain will be reached at an electric field of 340 MV/m. Attempting

to reach this condition by increasing the field beyond the maximum of 281 MV/m, shown here, resulted in a rapid degradation of the BiFeO<sub>3</sub> capacitors, including visible changes in the top electrode structure and electrical breakdown. Based on this estimate, however, we find that the fields we have already reached are close to the phase transition and that the required fields are within the range of present experimental tools. It may be difficult to reach and exploit the full rhombohedral-to-tetragonal phase transition in high-repetition rate experiments, which we hypothesize will be accompanied by the dissipation of mechanical energy. High electric fields will, however, now provide the means to tune and test the properties of BiFeO<sub>3</sub> through a wide range of responses without artifacts associated with variations in sample fabrication across a wide range of substrates.

This work was supported by NSF through Grant Nos. DMR-1106050 and OISE-0844424 (PE), and by the Army Research Office through Grant W911NF-10-1-0362 (CBE). Use of the Advanced Photon Source was supported by the U.S. Department of Energy, Office of Science, Office of Basic Energy Sciences, under Contract No. DE-AC02-06CH11357. The SPring-8 measurement was supported by the JASRI under proposal No. 2010B1663. J.Y.J. acknowledges support from the National Research Foundation of Korea (NRF) via MEST (Grant Nos. 2011-0009968 and 220-2011-1-C00016) and the Ministry of Knowledge Economy (MKE), Korea Institute for Advancement of Technology (KIAT) through the Inter-ER Cooperation Projects.

<sup>1</sup>L. Chen, V. Nagarajan, R. Ramesh, and A. L. Roytburd, *J. Appl. Phys.* **94**, 5147 (2003).

<sup>2</sup>S. Lisenkov, D. Rahmedov, and L. Bellaiche, *Phys. Rev. Lett.* **103**, 047204 (2009).

<sup>3</sup>M. Iwata and Y. Ishibashi, *Jpn. J. Appl. Phys.*, Part 1 **44**, 3095 (2005).

<sup>4</sup>D. Damjanovic, *IEEE Trans. Ultrason. Ferroelectr. Freq. Control* **56**, 1574 (2009).

<sup>5</sup>J. X. Zhang, B. Xiang, Q. He, J. Seidel, R. J. Zeches, P. Yu, S. Y. Yang, C. H. Wang, Y. H. Chu, L. W. Martin *et al.*, *Nat. Nanotechnol.* **6**, 97 (2011).

<sup>6</sup>S. Fujino, M. Murakami, V. Anbusathaiah, S. H. Lim, V. Nagarajan, C. J. Fennie, M. Wuttig, L. Salamanca-Riba, and I. Takeuchi, *Appl. Phys. Lett.* **92**, 202904 (2008).

<sup>7</sup>H. W. Jang, S. H. Baek, D. Ortiz, C. M. Folkman, R. R. Das, Y. H. Chu, P. Shafer, J. X. Zhang, S. Choudhury, V. Vaithyanathan *et al.*, *Phys. Rev. Lett.* **101**, 107602 (2008).

<sup>8</sup>R. J. Zeches, M. D. Rossell, J. X. Zhang, A. J. Hatt, Q. He, C. H. Yang, A. Kumar, C. H. Wang, A. Melville, C. Adamo *et al.*, *Science* **326**, 977 (2009).

<sup>9</sup>C. B. Eom, R. J. Cava, R. M. Fleming, J. M. Phillips, R. B. Vandover, J. H. Marshall, J. W. P. Hsu, J. J. Krajewski, and W. F. Peck, *Science* **258**, 1766 (1992).

<sup>10</sup>R. R. Das, D. M. Kim, S. H. Baek, C. B. Eom, F. Zavaliche, S. Y. Yang, R. Ramesh, Y. B. Chen, X. Q. Pan, X. Ke *et al.*, *Appl. Phys. Lett.* **88**, 242904 (2006).

<sup>11</sup>A. Grigoriev, R. Sichel, H. N. Lee, E. C. Landahl, B. Adams, E. M. Dufresne, and P. G. Evans, *Phys. Rev. Lett.* **100**, 027604 (2008).

<sup>12</sup>O. Sakata, Y. Furukawa, S. Goto, T. Mochizuki, T. Uruga, K. Takeshita, H. Ohashi, T. Ohata, T. Matsushita, S. Takahashi *et al.*, *Surf. Rev. Lett.* **10**, 543 (2003).

<sup>13</sup>J. Wang, J. B. Neaton, H. Zheng, V. Nagarajan, S. B. Ogale, B. Liu, D. Viehland, V. Vaithyanathan, D. G. Schlom, U. V. Waghmare *et al.*, *Science* **299**, 1719 (2003).

<sup>14</sup>R. J. Sichel, Ph.D. dissertation, University of Wisconsin, 2011.

<sup>15</sup>V. V. Shvartsman, W. Kleemann, R. Haumont, and J. Kreisel, *Appl. Phys. Lett.* **90**, 172115 (2007).

<sup>16</sup>M. Holt, P. Zschack, H. Hong, M. Y. Chou, and T.-C. Chiang, *Phys. Rev. Lett.* **86**, 3799 (2001).

<sup>17</sup>M. Holt, M. Sutton, P. Zschack, H. Hong, and T.-C. Chiang, *Phys. Rev. Lett.* **98**, 065501 (2007).

<sup>18</sup>O. Diéguez, O. González-Vázquez, J. Wojdeł, and J. Íñiguez, *Phys. Rev. B* **83**, 094105 (2011).

<sup>19</sup>S. E. Park and T. R. ShROUT, *J. Appl. Phys.* **82**, 1804 (1997).

<sup>20</sup>S. Trolier-McKinstry, N. B. Gharb, and D. Damjanovic, *Appl. Phys. Lett.* **88**, 202901 (2006).